

FUNCTIONAL NETWORK IN NAVIGATION SATELLITE CLOCK ERROR PREDICTION

A Novel Application

Ying Wang¹, Bo Xu^{1,2} and Xuhai Yang³

¹College of Astronautics, Nanjing University of Aeronautics and Astronautics, Yudao street, Nanjing, China

²School of Astronomy & Space Science, Nanjing University, Nanjing, China

³National Time Service Centre, Xi'an, China

Keywords: Functional network, Time delay, Satellite clock error, Clock error prediction, Neural network.

Abstract: In order to describe the characteristics of navigation satellite clock error better and improve navigation satellite clock error prediction accuracy, a satellite clock prediction method based on functional network is proposed in this paper. The method added delay variables to the traditional functional network which can reflect the dynamical characteristics of navigation satellite clock error better than the traditional method without delay variables. The GPS satellites are taken for example; simulation results show that the prediction accuracy of the proposed method is better than those of quadratic polynomial, quadratic polynomial with periodic term, ARIMA and the grey methods.

1 INTRODUCTION

The performance of a navigation satellite are related to the behaviour of the atomic clocks hosted on the satellite; the real-time and reliable prediction of the behaviour of such clocks is needed to provide precise navigation performances and to optimize the interval between uploading of the corrections to the satellite clocks. Take Global Navigation Satellite System (GNSS) for example, the IGS, along with a multinational membership of organizations and agencies, provides GPS orbits and clocks, tracking data, and other high-quality GPS data and data products online to meet the objectives of a wide range of scientific and engineering applications and studies. The accuracy of the satellite and station clocks is announced to be better than 0.1 ns, while the orbits' accuracy to be less than 5 cm (Delporte, 2004). In fact, these high-accuracy data are not available in real time but a posteriori, with a delay up to 13 days, while the broadcast ephemeris is realized in real time which accuracy reaches 5 ns.

Many papers have dealt with the prediction problem. Zhang et al. (2007) constructed a model which includes a quadratic polynomial and the periodic terms. Cui and Jiao (2005) introduced the grey system into the research on the prediction of the

clock error of the navigation satellite and obtained better results. Xu and Zeng (2009) proposed a new ARIMA (0, 2, q) model to predict the clock error and gained a series of important achievements. However, further studies show that there exist some limitations in the classical methods of navigation satellite clock error prediction. On the basis of exploration of the limitations of the satellite clock error prediction conducted by means of the traditional models, we present a novel research on the navigation satellite clock error prediction based on functional network.

Castillo et al. (1999) introduced functional network as a generalization of the standard neural network. Unlike neural networks that are basically driven by data, functional network may be considered more as problem-driven models than as data-driven models. Functional networks have been successfully demonstrated in some sample applications, e.g. to extract information masked by chaos (Castillo and Gutierrez, 1998), and have been used for nonlinear system identification (Li et al., 2001). It has also been used for predicting fresh and hardened properties of self-compacting concretes (Tomasiello, 2011).

In this paper, we apply an alternative new approach using functional networks in navigation satellite clock error prediction. And, the results are

used to compare with the conventional grey method (GM), the quadratic polynomial method (QPM), the quadratic polynomial with periodic term method (QPPTM) and the autoregressive integrated moving average method (ARIMA). The paper is organized as follows: Section 2 is a brief description of functional network. The functional network used in this study is demonstrated and its mathematical representation is presented in detail. Section 3 describes the atomic clock error prediction model based on functional network, while the mathematical model of atomic clock error is combined with and derived. Section 4, five separate tests were carried out on the materials of the GPS satellite clock error of 20 different and continuous time intervals. The results are shown in Section 5, where the models' ability to predict satellite atomic clock error at different time intervals are compared. Some diagrams from the simulation are presented in that section. The final conclusions are presented in Section 6.

2 FUNCTIONAL NETWORK

Figure 1 shows a typical architecture of a functional network illustrating its main components. A functional network consists of several elements including: one layer of input storing neurons, one layer of output storing neurons, one (or more) layers of processing neurons, optional layers of intermediate storing neurons, and a set of direct links between them (Castillo, 1998).

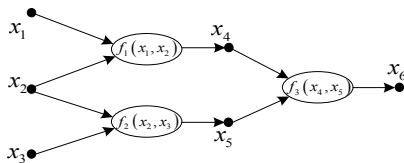


Figure 1: Functional network architecture.

A processing neuron receives a set of input signals coming from the previous layer and delivers the result of its calculation to the next layer following the direction of the links. Each processing neuron is associated with a function, which can be multivariate and can have as many arguments as there are inputs to the neuron. The input, output, or intermediate information produced by processing neurons is stored in storing neurons. The functions associated with processing neurons are the key to functional networks. Unlike artificial neural networks, in functional networks, neuron functions are unknown (arbitrary) functions from given

families that must be determined during the training process. There are no weights in functional networks as their function in ANN is now incorporated into the neuron functions.

To work with functional networks, in addition to the data information, it is important to understand the problem to be solved since the selection of the topology of a functional network is normally based on the properties which usually lead to a clear and single network structure. From the different possible functional network forms, the separable functional network is a simple family with many applications. It uses a functional expression that combines the separated efforts of input variables. In this study, our goal is to predict atomic clock error using both the current time and the atomic clock error at previous time steps as inputs. The separable functional network may be used as the approximate model in atomic clock error prediction on the basis of the physical model of the atomic clock.

2.1 Separable Functional Network

In this section, we demonstrate a simple separable functional network with two inputs and one output. Figure 2 depicts the topology of a separable functional network. The relationship between z , x and y can be defined mathematically as follows,

$$z = F(x, y) = \sum_{i=1}^n f_i(x)g_i(y) \tag{1}$$

where x , y are the two input variables and z is the output of the functional network. $f_i(\cdot)$, $g_i(\cdot)$ are the unknown neuron functions.

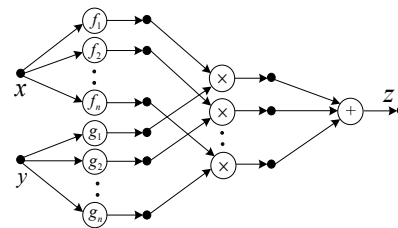


Figure 2: The general separable functional network architecture.

2.2 The Uniqueness of Representation

Before using functional networks, it is important to make sure of the uniqueness of the representation of the network in order to obtain a more general set of functions satisfying a given network topology. This is due to the danger that, in some cases, different neuron functions may lead to exactly the same

output for the same input thereby leading to an ill-conditioned estimation problem (Bruen and Dooge, 1984). To address this problem, Castillo and Gutierrez have given a general solution (Theorem 1) for all the functional networks of Eq. (1) as follows:

Theorem 1. All solutions of equation $\sum_{i=1}^n f_i(x)g_i(y)=0$ can be written in the form $f(x)=\mathbf{A}\boldsymbol{\varphi}(x)$, $g(y)=\mathbf{B}\boldsymbol{\psi}(y)$, where \mathbf{A} and \mathbf{B} are constant matrices (of dimensions $n \times r$ and $n \times (n-r)$, respectively) with $\mathbf{A}^T \mathbf{B} = 0$, and $\boldsymbol{\varphi}(x) = (\varphi_1(x), \dots, \varphi_r(x))$, $\boldsymbol{\psi}(y) = (\psi_{r+1}(y), \dots, \psi_n(y))$ are two arbitrary systems of mutually linearly independent functions, and r is an integer between 0 and n .

It is important to notice that an initial value for the neuron function(s) has to be assigned to represent the uniqueness conditions.

In this study we start with the simplest network structure by assuming $g_1 = f_2 = 1$ with $n = 2$. Then, Eq. (1) can be simplified to

$$z = F(x, y) = f(x) + g(y) \quad (2)$$

2.3 Training

Training is an important stage in the application of a functional network. It is also equivalent, in practice, to the fitting process in conventional methods of modelling. The process of training the functional network associated with Eq. (2) is equivalent to estimating the neuron functions $f(\cdot)$ and $g(\cdot)$ from the available data. The objective is to minimize an error function that measures the difference between the model output \hat{z} and the actual (measured) values z .

From Theorem 1, we can approximate the neuron functions by considering a linear independent combination of a standard form for each neuron function. The standard functional form (φ_j, ψ_j) can be a polynomial family, a Fourier series, or any other set of linearly independent functions. Therefore, the neuron functions can be expressed as

$$\hat{f}(x) = \sum_{j=1}^p a_j \varphi_j(x) \quad (3)$$

$$\hat{g}(y) = \sum_{j=1}^q b_j \psi_j(y) \quad (4)$$

For a clearer presentation in the following calculations, we use the same parameter symbols for Eq. (3) and (4), and rewrite Eq. (4) as

$$\hat{g}(y) = \sum_{j=p+1}^{p+q} a_j \varphi_{j-p}(y) \quad (5)$$

where the coefficients a_j are the parameters of the functional networks, and p, q are the orders of either the polynomial family or Fourier series. The objective function used here is the sum of square errors, which should be minimized,

$$Q = \sum_{i=1}^k \hat{e}^2 = \sum_{i=1}^k [z_i - \hat{f}(x_i) - \hat{g}(y_i)]^2 \quad (6)$$

where k is the training sample size. For a unique representation of the functional networks, we must add an initial functional condition. In this case we can use either of the two initial conditions,

$$f(x_0) = u \quad (7)$$

$$g(y_0) = v \quad (8)$$

where x_0, y_0 and u, v are given constants. Therefore, we use Eq. (7) as a penalty term adding to the objective function (Eq. (6)). Using a Lagrange multiplier, Eq. (6) becomes

$$Q_\lambda = Q + \lambda (\hat{f}(x_0) - u) \quad (9)$$

where λ is a constant. Minimization of the above function Q_λ is equivalent to solving the set of derivative equations of Q_λ with respect to parameters a_j and multiplier λ . Then, we have

$$\frac{\partial Q_\lambda}{\partial a_r} = -2 \sum_{i=1}^k \left[z_i - \sum_{j=1}^p a_j \varphi_j(x_i) - \sum_{j=p+1}^{p+q} a_j \varphi_{j-p}(y_i) \right] \varphi_r(x_i) + \lambda \varphi_r(x_0) = 0, r = 1, \dots, p \quad (10)$$

$$\frac{\partial Q_\lambda}{\partial a_r} = -2 \sum_{i=1}^k \left[z_i - \sum_{j=1}^p a_j \varphi_j(x_i) - \sum_{j=p+1}^{p+q} a_j \varphi_{j-p}(y_i) \right] \varphi_{r-p}(y_i) = 0, r = p+1, \dots, p+q \quad (11)$$

$$\frac{\partial Q_\lambda}{\partial \lambda} = \sum_{j=1}^p a_j \varphi_j(x_0) - u = 0, r = 1, \dots, p \quad (12)$$

This leads to a system of $p+q+1$ linear equations where the unknown coefficients are parameters a_j and λ .

3 THE CLOCK ERROR PREDICTION MODEL BASED ON FUNCTIONAL NETWORK

3.1 The Mathematical Model of Atomic Clock Error

The clock signal is typically affected by five random noises that are known in metrological literature as white phase noise (WPN), flicker phase noise (FPN), white frequency noise (WFN) that produces a Brownian motion (BM) (also called Wiener process or random walk) on the phase, flicker frequency noise (FFN) and random white frequency noise (RWFN), which produces an integrated Brownian motion (IBM) on the phase. The presence of different kinds of random noises and their entity is different from clock to clock. From experimental evidence it appears that on the caesium clock the predominant noises are the WFN and the RWFN that correspond in mathematical language to the Wiener process and to the integrated Wiener process, respectively, on the phase deviation. Denoting by $X_1(t)$ the atomic clock phase deviation, its time evolution can be written as a dynamical system of stochastic differential equation as (Panfilo and Tavella, 2008)

$$\begin{cases} dX_1(t) = X_2(t) \cdot dt + \sigma_1 dW_1(t), \\ dX_2(t) = d \cdot dt + \sigma_2 dW_2(t) \end{cases} \quad (13)$$

with initial conditions $X_1(0) = x_0, X_2(0) = y_0$, which represent the initial phase and frequency deviation. The constant d indicates the frequency aging or drift. The triplet (x_0, y_0, d) represents what is generally referred to as the deterministic phenomena of the atomic clocks. The positive constants σ_1 and σ_2 represent the diffusion coefficients of the two noise components W_1 and W_2 , while indicate the intensity of each noise. $W_1(t)$ is the Wiener noise acting on the phase deviation X_1 and corresponding to a WFN; the Wiener process can, in fact, be thought of as the integral of a white noise. $W_2(t)$ represents the Wiener process acting on the frequency (the so-called 'random walk FN') and yields to an integrated Wiener process on the phase. The Wiener process $\{W(t), t \geq 0\}$ is defined as a Gaussian process that starts from $\{W(0) = 0\}$ and then at any instant has a probability distribution

given by $N(0, t)$ with a zero mean value and variance equal to t .

Note that X_1 represents the phase deviation, while the frequency deviation results in \dot{X}_1 . The second component X_2 is only a part of the clock frequency deviation, i.e. what is generally called the 'random walk' frequency component.

Since Eq. (13) is a complete strictly linear stochastic differential equation, it is possible to obtain its solution in closed form as

$$\begin{cases} X_1(t) = x_0 + y_0 t + d \cdot \frac{t^2}{2} + \sigma_1 W_1(t) + \sigma_2 \int_0^t W_2(s) ds, \\ X_2(t) = y_0 + d \cdot t + \sigma_2 W_2(t). \end{cases} \quad (14)$$

Let us now consider a fixed time interval T' and an equally spaced partition $0 \equiv t_0 < t_1 < \dots < t_N \equiv T'$ and let us denote the resulting discretization step with $\tau = t_{k+1} - t_k$, for each $k = 0, 1, \dots, N-1$. We can express solution Eq. (14) at epoch t_{k+1} in terms of the process at epoch t_k as

$$\begin{cases} X_1(t_{k+1}) = X_1(t_k) + X_2(t_k) \tau + d \cdot \frac{\tau^2}{2} + J_{k,1}, \\ X_2(t_{k+1}) = X_2(t_k) + d \cdot \tau + J_{k,2}. \end{cases} \quad (15)$$

where the vector J_k is normally distributed as

$$J_k \sim N \left(\mathbf{0}, \begin{bmatrix} \sigma_1^2 \tau + \sigma_2^2 \frac{\tau^3}{3} & \sigma_2^2 \frac{\tau^2}{2} \\ \sigma_2^2 \frac{\tau^2}{2} & \sigma_2^2 \tau \end{bmatrix} \right) \quad (16)$$

The measured values of atomic clock error $X(t_{k+1})$ is

$$\begin{aligned} X(t_{k+1}) &= X_1(t_{k+1}) + \varepsilon(t_{k+1}) \\ &= X_1(t_k) + X_2(t_k) \tau + d \cdot \frac{\tau^2}{2} + J_{k,1} + \varepsilon(t_{k+1}) \end{aligned} \quad (17)$$

where $\varepsilon(t)$ is the Gaussian measurement noise with $\varepsilon(t) \sim N(0, \sigma^2)$. Finally, the mathematical model of atomic clock error can be written as

$$X(t_{k+1}) = X(t_k) + X_2(t_k) \tau + d \cdot \frac{\tau^2}{2} + \int_{t_k}^{t_{k+1}} f(t) dt \quad (18)$$

where $\tau = t_{k+1} - t_k$, $X(t_{k+1})$ is the navigation satellite clock error at the time of t_{k+1} , $X(t_k)$ is the satellite clock error at the referent time of t_k , $X_2(t_k)$ is the frequency deviation of clock at the referent time of t_k , d is the frequency aging or drift of clock at the

referent time of t_k and $\int_{t_k}^{t_{k+1}} f(t)dt$ is a kind of random clock error caused by the random error of frequency, of which the statistical characteristics can be described only through the degree of stability of the clock and the concrete value can not be known.

Since the traditional QPM neglects the stochastic component during the clock error model building, and the GM can not make full use of existing clock error data, the identification of the ARIMA is relatively difficult. Thus the precision of clock error prediction of these traditional models is low. According to the present research situations, we apply functional network in navigation satellite clock error prediction, while both the trend item and the stochastic component of the atomic clock error are considered comprehensively.

3.2 The Clock Error Prediction Model based on Functional Network

In this paper we use both the current time and the atomic clock error at previous time steps as inputs, and use the current clock error as output of the prediction model. This method of modelling makes the functional network fully study the dynamic characteristic of the historical data of the clock error, and avoid the disadvantage of QPM, which is the error accumulation become more and more obvious with the lapse of time, while QPM simply uses time as input. Figure 3 shows the structure of the model of the train stage.

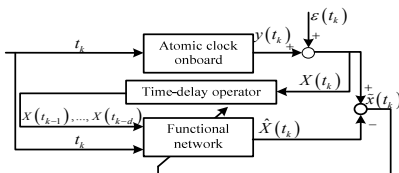


Figure 3: Diagram of satellite clock error train structure based on functional network.

where t_k represents current time, $y(t_k)$ represents the navigation satellite clock error at current time, $\varepsilon(t_k)$ is the measurement error, $X(t_k)$ represent the actual observed value of the clock error at current time, $X(t_{k-1}), \dots, X(t_{k-d})$ represent the clock errors at previous time steps. The inputs of functional network are t_k and $X(t_{k-1}), \dots, X(t_{k-d})$, the output is $\hat{X}(t_k)$, which is the prediction value of clock error at current time, $\tilde{x}(t_k)$ is the prediction error at current time. During the training process, the

functional network approximates the functional relationship expressed as:

$$\begin{aligned} \hat{X}(t_k) &= F(t_k, X(t_{k-1}), \dots, X(t_{k-d})) \\ &= \hat{f}_t(t) + \sum_{k=1}^d \hat{f}_k(x_{t-k}) \end{aligned} \quad (19)$$

where $\hat{f}_t(t)$, which is the contribution of current time, denotes the trend item, and $\sum_{k=1}^d \hat{f}_k(x_{t-k})$, which is the combination of the contributions of the clock errors at previous time steps, denotes the stochastic component of the atomic clock error.

We adopt the method of non-mechanism modelling, using current time and history data of clock error and high non-linear mapping of functional network, the input-output relationship of practical system of the atomic clock error is simulated and the model which has been set by training can be used in the prediction stage, the structure of the model of this stage is shown in Figure 4.

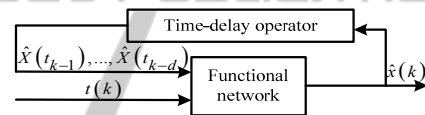


Figure 4: Diagram of satellite clock error prediction structure based on functional network.

Considering the mathematical model of atomic clock error, we choose the polynomial family for the standard functional form (φ_j, ψ_j) . In addition, an initial condition function $f(x_0) = u$ is assigned in order to obtain the unique representation.

4 APPLICATION TO NAVIGATION SATELLITE CLOCK ERROR PREDICTION

In order to verify the feasibility and effectiveness of this method, we carried out five separate tests on the clock error prediction, and compared its performance with the other four conventional methods, which are the GM, QPM, QPPTM and ARIMA. To ensure obtaining reliable model comparisons, we used the GPS satellite clock error of 20 different and continuous time intervals for each test, and the materials of the GPS clock error, which were used in the tests, are the precise satellite clock solutions published by IGS with five minutes sampling interval. For the data pre-process,

according to the anomalies and missing values of the atomic clock error, firstly we performed integrity check on the data, and then adopted Baarda data detection method in anomaly detection, finally used Lagrange interpolation interpolates these data after the anomalies removal.

The available data for each test was divided into two groups: training (calibration) set A , and testing (validation) set B . The GM, QPM, QPPTM, ARIMA and FN were fitted to the calibration data, where the GM adopted the same modelling scheme as Cui and Jiao (2005), which used the 8 initial epochs before the prediction time for modelling; The QPPTM reduced the noise of the residuals on the basis of quadratic fitting, which was realized by utilizing the spectrum analysis; The ARIMA model's order determination was completed by Bayesian information criterion (BIC). As for the FN model, due to the dynamic characteristic of clock error of different satellite is not the same at the different time interval, to make precisely prediction, we chose a set of candidate networks, with the num of input nodes from 2 to 5, and the num of basis functions which combine the processing neuron of FN from 2 to 5, here once again the calibration set A was divided into two groups: training (calibration) set A' and testing (validation) set B' . The candidate model structures were fitted to the calibration data A' , and were predicted to the validation data B' ; the best performing model from them was selected to represent them, and would be fitted to the calibration set A , which was the same step as others.

Five separate simulation prediction tests were carried out; the simulation results would be given in diagrams. Considering that different kinds of atomic clock onboard may have differences, both the figures of error curve of PRN10 and PRN11 were given, of which both the start time of prediction is January 8, 2009, where PRN10 is the satellite equipped with the caesium clock and PRN11 is the satellite equipped with the rubidium clock. In addition, the average values of prediction errors of each satellite of 20 different time intervals would be given, and discussions would be carried out according to different kinds of atomic clocks onboard. The concrete contents of tests are as follows.

Test 1: 6 hours prediction test was carried out, adopting the above five methods and utilizing the GPS satellite clock error of 20 different and continuous time intervals. The time interval of simulation spanned from January 7 to 11, 2009. The simulation results was shown in Figure 5, and the

average values of prediction errors of each satellite of 20 different time intervals, which were obtained by five methods is summarized in Table 1.

Test 2: 12 hours prediction test was carried out, adopting the above five methods and utilizing the GPS satellite clock error of 20 different and continuous time intervals. The time interval of simulation spanned from January 7 to 16, 2009. The simulation results was shown in Figure 6, and the average values of prediction errors of each satellite of 20 different time intervals, which were obtained by five methods is summarized in Table 2.

Test 3: 1 day prediction test was carried out, adopting the above five methods and utilizing the GPS satellite clock error of 20 different and continuous time intervals. The time interval of simulation spanned from January 7 to 27, 2009. The simulation results was shown in Figure 7, and the average values of prediction errors of each satellite of 20 different time intervals, which were obtained by five methods is summarized in Table 3.

Test 4: 7 days prediction test was carried out, adopting the above five methods and utilizing the GPS satellite clock error of 20 different and continuous time intervals. The time interval of simulation spanned from January 7 to February 2, 2009. The simulation results was shown in Figure 8, and the average values of prediction errors of each satellite of 20 different time intervals, which were obtained by five methods is summarized in Table 4.

Test 5: 14 days prediction test was carried out, adopting the above five methods and utilizing the GPS satellite clock error of 20 different and continuous time intervals. The time interval of simulation spanned from January 7 to February 9, 2009. The simulation results was shown in Figure 9, and the average values of prediction errors of each satellite of 20 different time intervals, which were obtained by five methods is summarized in Table 5.

5 RESULTS AND DISCUSSIONS

For the test 1 (6 hours prediction), Table 1 demonstrates the performances of the five methods in terms of average errors of 20 different time interval, since the QPM can make full use of existing clock error data, which has a good reflection of the whole change rule of the clock error, the prediction precision of which is equivalent with the GM's except PRN27. The QPPTM considers the characteristics of the periodical changes on the basis of the QPM, so the prediction precision is better than the latter's. The prediction precision of functional

network is superior to those of the other four methods', except that the prediction precision of PRN11 and PRN24 are equivalent with the others.

For the test 2 and test 3 (12 hours prediction and 1 day prediction), the prediction precisions of the QPM and the QPPTM are overall superior to that of the GM. Due to the identification of the ARIMA is relatively difficult, the prediction performance of ARIMA is unstable, where the optimal prediction precision of the ARIMA for 12 hours prediction is 0.8 ns , while the poorest can reach up to the order of μs . The prediction precision of functional network is superior to those of the other four methods', except that the prediction precisions of PRN 28 in 12 hours prediction and PRN32 in 1 day prediction are equivalent with the others.

For the test 4 (7 days prediction), compared with the other four methods, the prediction precision of functional network totally has improvement, with the average values of the prediction error is 0.4 percent of other methods' under the best situation, and 95.2 percent of other methods' under the poorest situation of improvement.

For the test 5 (14 days prediction), the analysis of the prediction precision between that of the QPM and the GM displays that owing to the characteristics of the error accumulation of the QPM, with the increase in the prediction time, the prediction precision of the GM is evidently superior to that of the QPM. Due to the influence of the QPM, which is the principle term, the QPPTM also shows the characteristics of the error accumulation, with slightly better than the QPM. The prediction precision of functional network totally has improvement compared with the other four methods', with the average values of the prediction error is 0.2 percent of other methods' under the best situation, and 93.6 percent of other methods' under the poorest situation of improvement.

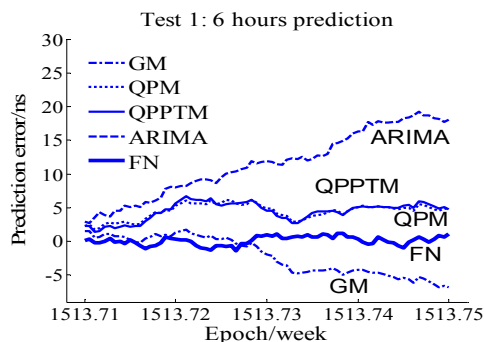


Figure 5(a): 6 Hours prediction error of PRN10.

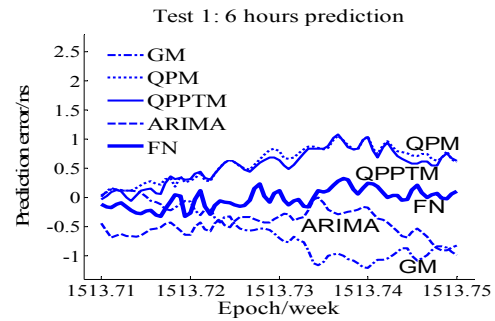


Figure 5(b): 6 Hours prediction error of PRN11.

From all the tests above, we can see that the prediction precision of functional network totally has improvement compared with the other four methods', especially for the test 4 and test 5, which are 7 days and 14 days prediction tests. In addition, the prediction precisions of the rubidium clock are superior to the caesium clock, which is true for all the methods in the five tests.

Table 1: Comparison among the 6 hours prediction accuracy (unit: ns).

Kind of clock onboard	PRN	GM	QP	QPPTM	ARIMA	FN
Caesium clock	03	5.14	5.07	5.00	10.0	4.78
	09	4.88	6.57	6.21	10.4	4.40
	10	7.30	4.12	3.98	47.6	3.20
	24	5.33	6.21	6.19	6.67	8.77
	27	7.38	16.80	16.7	16.5	9.71
Rubidium clock	30	8.09	8.29	8.22	9.98	4.17
	02	0.73	0.59	0.58	1.75	0.34
	04	1.81	1.78	1.77	13.4	1.21
	07	0.70	0.83	1.11	1.06	0.56
	11	0.68	0.64	0.63	0.66	0.70
	12	1.08	1.62	1.59	1.93	0.63
	13	0.88	0.88	0.87	1.22	0.52
	14	0.77	0.83	0.81	2.91	0.43
	15	1.09	0.58	0.57	4.05	1.01
	16	1.06	1.41	1.37	3.11	0.68
	17	0.92	0.38	0.37	1.82	0.33
	18	0.98	0.86	0.84	1.79	0.52
19	0.75	0.64	0.63	0.91	0.36	
20	1.17	1.09	1.08	1.74	0.35	
21	1.24	0.97	0.94	1.58	0.58	
22	2.35	1.21	1.20	1.18	0.65	
23	0.67	0.56	0.54	0.93	0.28	
28	0.93	0.97	0.96	66.6	0.63	
29	0.67	0.71	0.70	1.10	0.37	
31	0.63	0.73	0.71	1.42	0.45	
32	1.45	3.53	3.51	4.56	1.83	

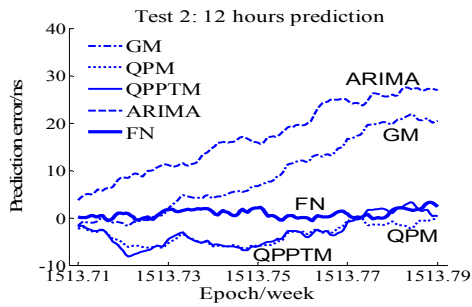


Figure 6(a): 12 Hours prediction error of PRN10.

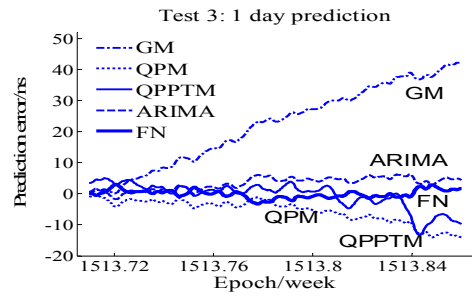


Figure 7(a): 1 Day prediction error of PRN10.

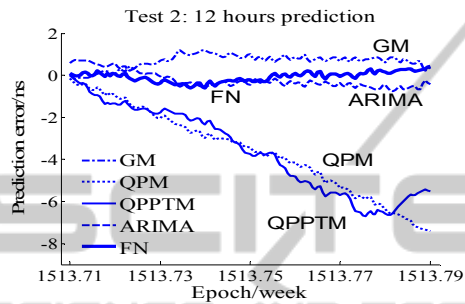


Figure 6(b): 12 Hours prediction error of PRN11.

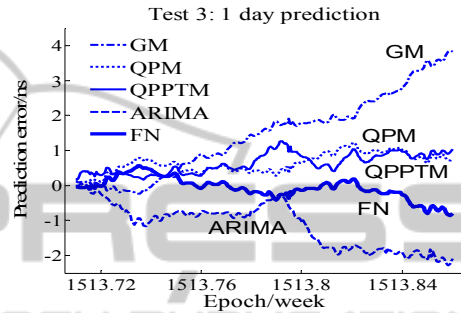


Figure 7(b): 1 Day prediction error of PRN11.

Table 2: Comparison among the 12 hours prediction accuracy (unit: ns).

Kind of clock onboard	PRN	GM	QP	QPPTM	ARIMA	FN
Caesium clock	03	10.6	11.4	11.3	7.52	5.25
	09	11.2	15.7	15.6	13.7	7.05
	10	12.6	8.31	8.27	9.69	5.90
	24	9.71	9.84	9.78	7.77	4.49
	27	18.7	27.0	26.7	50.5	8.25
	30	17.6	16.1	16.0	45.2	6.48
Rubidium cloc	02	1.77	1.34	1.35	0.81	0.47
	04	3.69	4.23	4.22	16.2	1.50
	07	1.26	0.95	0.94	1.08	0.51
	11	1.35	2.66	2.65	2.28	0.39
	12	1.82	2.33	2.31	1.93	0.53
	13	1.39	1.56	1.55	1.84	0.60
	14	1.53	0.90	0.87	2.86	0.51
	15	1.41	1.23	1.22	3.99	1.01
	16	1.51	1.83	1.80	2.32	0.37
	17	2.03	1.17	1.16	1.09	0.43
	18	2.05	1.02	1.00	2.86	0.44
	19	1.43	1.21	1.19	1.44	0.44
	20	2.10	1.16	1.14	1.85	0.55
	21	2.57	1.61	1.60	1.98	0.62
	22	3.57	1.46	1.44	1.11	0.89
	23	1.66	0.75	0.73	0.87	0.37
28	2.01	1.91	1.90	1.10	2.03	
29	1.08	1.08	1.07	1.39	0.61	
31	1.37	1.47	1.47	2.29	0.64	
32	3.21	3.45	3.39	10.4	1.96	

Table 3: Comparison among the 1 day prediction accuracy (unit: ns).

Kind of clock onboard	PRN	GM	QP	QPPTM	ARIMA	FN
Caesium clock	03	22.7	13.1	13.0	15.5	6.38
	09	21.37	15.38	15.32	99.7	8.23
	10	16.5	12.9	12.8	13.0	6.98
	24	24.4	13.0	12.9	8128	5.98
	27	34.7	15.8	15.4	41.3	14.9
	30	26.81	14.2	14.1	6196	7.52
Rubidium clock	02	3.29	1.33	1.32	1.69	0.64
	04	6.26	3.31	3.20	20.8	1.72
	07	2.80	1.79	1.78	1.55	0.90
	11	2.88	0.95	0.94	3.02	1.33
	12	2.97	1.22	1.20	2.93	0.58
	13	2.77	1.63	1.60	2.43	0.85
	14	3.30	1.37	1.36	4.56	0.82
	15	3.02	1.94	1.93	17.7	1.53
	16	4.89	0.74	0.68	7.05	0.56
	17	3.40	1.70	1.69	2.52	1.34
	18	3.24	0.94	0.92	3.96	0.54
	19	2.49	1.56	1.55	1.80	0.79
	20	4.54	1.64	1.60	2.67	0.66
	21	8.36	1.50	1.49	2.17	0.75
	22	5.61	3.13	3.12	3.31	2.33
	23	2.86	0.91	0.90	1.43	0.66
28	5.01	5.50	5.48	4.64	4.90	
29	2.42	2.00	1.98	3.56	1.39	
31	2.86	2.26	2.26	2.74	1.39	
32	5.19	2.44	2.40	20.49	2.66	

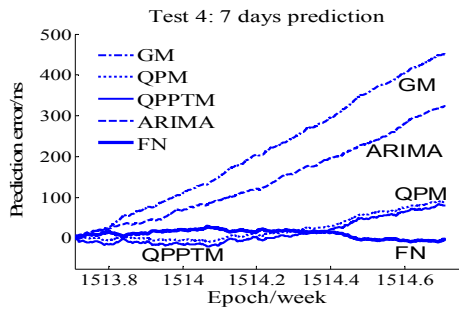


Figure 8(a): 7 Days prediction error of PRN10.

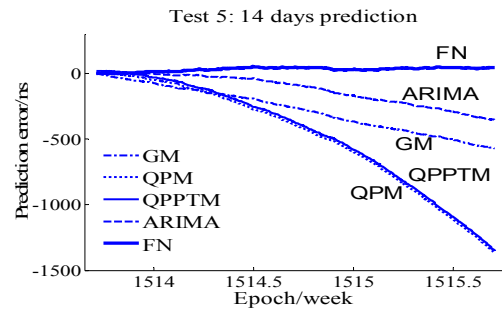


Figure 9(a): 14 Days prediction error of PRN10.

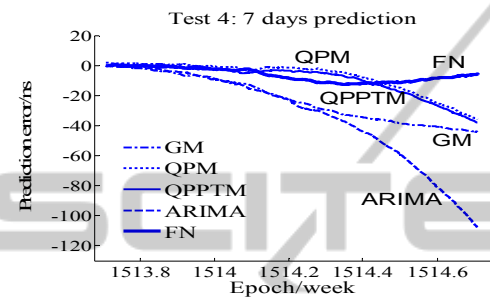


Figure 8(b): 7 Days prediction error of PRN11.

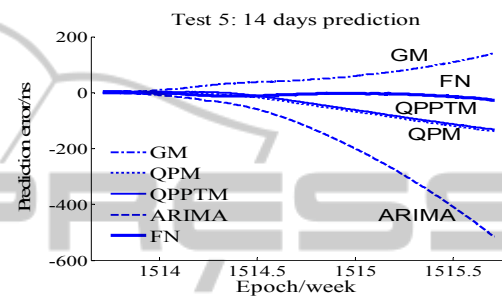


Figure 9(b): 14 Days prediction error of PRN11.

Table 4: Comparison among the 7 days prediction accuracy (unit: ns).

Kind of clock onboard	PRN	GM	QP	QPPTM	ARIMA	FN
Caesium clock	03	150.5	290.6	290.9	227.1	27.65
	09	146.6	308.9	309.0	2118	37.51
	10	127.2	223.2	220.2	283.7	28.80
	24	172.4	251.4	250.9	804	27.8
	27	275	334	330	852	33.0
	30	176	313	312	504	30.53
Rubidium clock	02	22.7	29.1	29.1	3112	11.5
	04	49.4	70.6	70.4	462	19.2
	07	20.9	38.7	38.6	35.7	8.36
	11	20.5	26.8	26.7	47.9	10.7
	12	25.8	22.4	21.4	50.2	8.51
	13	20.4	35.7	35.4	38.1	5.71
	14	32.8	27.9	27.2	39.8	5.85
	15	24.8	41.0	40.0	352	9.09
	16	30.5	14.5	14.4	66.2	5.01
	17	29.7	40.3	40.4	635	17.8
	18	23.1	21.1	21.0	89.3	3.79
	19	18.8	30.3	30.2	23.7	4.86
	20	31.5	36.7	36.2	38.2	5.81
	21	54.2	28.2	28.0	39.8	5.28
	22	50.9	78.2	78.0	67.9	34.2
	23	20.0	15.3	14.8	17.0	5.06
28	31.2	123	121	859	29.7	
29	36.6	33.6	33.4	156	20.1	
31	20.74	54.11	40.85	60.09	12.99	
32	33.30	41.23	40.80	412.7	23.66	

Table 5: Comparison among the 14 days prediction accuracy (unit: ns).

Kind of clock onboard	PRN	GM	QP	QPPTM	ARIMA	FN
Caesium clock	03	295.7	1058	1059	1e+4	71.46
	09	304.9	1108	1108	2e+4	83.66
	10	264	824	823	4e+5	49.1
	24	350	914	912	8e+3	59.6
	27	659	1201	1195	4e+5	62.8
	30	355	1140	1132	3e+5	77.4
Rubidium clock	02	52.49	107.5	107.6	4e+3	44.19
	04	115	254	250	1e+3	11.0
	07	44.6	139	139	206	20.7
	11	46.1	106	106	351	23.7
	12	69.8	80.7	80.5	301	38.1
	13	43.8	131	130	166	13.9
	14	92.6	102	101	309	18.8
	15	73.6	143	141	2e+3	34.4
	16	56.9	51.7	51.0	448	16.4
	17	62.9	138	135	596	36.8
	18	50.1	77.1	76.5	300	11.0
	19	39.6	107	106	119	13.7
	20	64.1	137.7	137.0	3e+4	17.2
	21	104.0	102.5	102.0	154.8	14.92
	22	96.2	269	265	292	69.9
	23	41.8	54.3	54.1	137	16.8
28	58.1	463	460	3e+4	54.4	
29	142	110	109	254	55.1	
31	39.6	198	136	211	29.2	
32	64.4	149	140	9e+4	57.4	

6 CONCLUSIONS

Functional network is considered as a generalization of artificial neural network, it is first introduced in the problem of clock error prediction, and delay variables are added to the traditional functional network. In this study, five separate simulation tests of the navigation satellite clock error prediction were carried out, and five models were applied to it, using the precise satellite clock solutions published by IGS with five minutes sampling interval as simulation data. The results of the simulation tests demonstrate that the functional network, which is added with delay variables, can reflect the dynamic characteristics of navigation satellite clock error better than the GM, QPM, QPPTM and ARIMA, as the prediction precision is better than the others, and can be used as a novel method in navigation satellite clock error prediction.

ACKNOWLEDGEMENTS

This work was supported by the National Science Foundation of China, 11078001 and 11033004.

REFERENCES

- Bruen, M., Dooge, J. C. I., 1984. An efficient and robust method for estimating unit hydrograph ordinates. *Journal of Hydrology*, vol.70, February, pp.1-24.
- Castillo, E., 1998. Functional Networks. *Neural Processing Letters*, 7, pp. 151-159.
- Castillo, E., Cobo. A., Gutiérrez J. M. et al., 1999. *Functional networks with applications: a neural-based paradigm*. Boston et al.: Kluwer Academic Publishers.
- Castillo, E., Gutiérrez, J. M., 1998. Nonlinear time series modeling and prediction using functional networks. Extracting information masked by chaos. *Physics Letters A*, 244, pp.71-84.
- Cui X. Q., Jiao W. H., 2005. Grey system model for the satellite clock error predicting. *Geomatics and Information Science of Wuhan University*, vol. 30, no. 5, May, pp.447-450.
- Delporte, J., 2004. Performance of GPS on board clocks computed by IGS, *Frequency and Time Forum*. EFTF 2004.18th European, Guildford, pp.201-207.
- Li C. G., Liao X. F., He S. B. et al., 2001. Functional network method for the identification of nonlinear system. *System Engineering and Electronics*, vol. 23, no. 11, pp.50-53.
- Panfilo, G., Tavella, P., 2008. Atomic clock prediction based on stochastic differential equations. *Metrologia* 45, vol.45, no.6, December, pp.108-110.
- Tomasiello, S., 2011. A functional network to predict fresh and hardened properties of self-compacting concretes. *International Journal for Numerical Methods in Biomedical Engineering*, vol. 27, no.6, June, pp.840-847.
- Xu J. Y., Zeng A.M., 2009. Application of ARIMA(0,2,q) model to prediction of satellite clock error. *Journal of Geodesy and Geodynamics*, vol. 29, no. 5, October, pp.116-120.
- Zhang B., Ou J. K., Yuan Y. B. et al., 2007. Fitting method for GPS satellite Clock errors using wavelet and spectrum analysis. *Geomatics and Information Science of Wuhan University*, vol.32, no.8, August, pp.715-718.